

**The structure, composition, and application of the cell envelope from  
*Caulobacter crescentus***

by

Michael D Jones

B. Science, Specialization in Biotechnology, University of Alberta, 2006

M. Science, Pharmaceutical Sciences, University of Alberta, 2008

A THESIS SUBMITTED IN PARTIAL FULFILLMENT  
OF THE REQUIREMENTS FOR THE DEGREE OF

**Doctor of Philosophy**

in

THE FACULTY OF SCIENCE

(Microbiology and Immunology)

The University Of British Columbia

(Vancouver)

April 2015

© Michael D Jones, 2015

# **Abstract**

This document provides brief instructions for using the `ubcdiss` class to write a -conformant dissertation in  $\text{\LaTeX}$ . This document is itself written using the `ubcdiss` class and is intended to serve as an example of writing a dissertation in  $\text{\LaTeX}$ . This document has embedded and is intended to be viewed using a computer-based reader.

Note: Abstracts should generally try to avoid using acronyms.

Note: at , both the () Ph.D. defence programme and the Library's online submission system restricts abstracts to 350 words.

# **Preface**

At , a preface may be required. Be sure to check the guidelines as they may have specific content to be included.

# Table of Contents

<b>Abstract</b> . . . . .	ii
<b>Preface</b> . . . . .	iii
<b>Table of Contents</b> . . . . .	iv
<b>List of Tables</b> . . . . .	vi
<b>List of Figures</b> . . . . .	vii
<b>List of Abbreviations</b> . . . . .	viii
<b>Acknowledgments</b> . . . . .	xi
<b>1 Introduction</b> . . . . .	1
1.1 S-layer structure . . . . .	1
1.2 History of S-layers . . . . .	1
<b>2 The core and O-polysaccharide structure of the <i>Caulobacter crescentus</i> lipopolysaccharide</b> . . . . .	5
2.1 Introduction . . . . .	5
2.2 Results . . . . .	6
2.2.1 Characterisation of whole LPS . . . . .	6
2.2.2 Initial assessment and component analysis . . . . .	6
2.2.3 O-antigen structure determination (PS1) . . . . .	7
2.2.4 Minor component determination . . . . .	12
2.2.5 Rhamnan polysaccharide determination (PS2) . . . . .	13
2.2.6 Core oligosaccharide determination . . . . .	13
2.3 Methods . . . . .	14
2.3.1 Bacterial strain construction and growth conditions . . . . .	14
2.3.2 LPS isolation . . . . .	15
2.3.3 Bligh Dyer Extraction . . . . .	17
2.3.4 Gel electrophoresis . . . . .	17

2.3.5	NMR spectroscopy . . . . .	17
2.3.6	LPS Chromatography . . . . .	17
2.3.7	Monosaccharide analysis . . . . .	18
2.3.8	Determination of absolute configurations of monosaccharides . . . . .	18
2.3.9	Methylation analysis . . . . .	18
2.3.10	Periodate oxidation . . . . .	18
2.4	Discussion . . . . .	19
<b>Bibliography</b>	. . . . .	<b>24</b>
<b>A Supporting Materials</b>	. . . . .	<b>27</b>

# List of Tables

Table 2.1	Nuclear magnetic resonance spectroscopy (NMR) data for <i>Caulobacter crescentus</i> ( <i>C. crescentus</i> ) polysaccharide (PS)1 (40°C) and deacylated PS1 (50°C). Me at 3.62/61.3 ppm. . . . .	21
Table 2.2	NMR data for the minor components of the double oxidized non-deacylated PS . . . . .	22
Table 2.3	NMR data for <i>C. crescentus</i> PS2 and its NaIO <sub>4</sub> oxidation product oligosaccharide (OS)1 . . . . .	23
Table 2.4	NMR data for the core oligosaccharide . . . . .	23

# List of Figures

Figure 1.1	Cross-sectional diagrams of the cell envelopes . . . . .	2
Figure 1.2	A simple overview of protein surface layer (S-layer) symmetries . . . . .	3
Figure 1.3	The first published image of a S-layer . . . . .	4
Figure 2.1	Visual comparison of <i>Escherichia coli</i> ( <i>E. coli</i> ) O122 lipopolysaccharide (LPS) and <i>Caulobacter crescentus</i> ( <i>C. crescentus</i> ) LPS . . . . .	6
Figure 2.2	Four different visualisations of <i>C. crescentus</i> LPS. . . . .	7
Figure 2.3	Matrix assisted laser desorption/ionization-time of flight mass spectroscopy (MALDI-TOF) analysis of intact, whole LPS from <i>C. crescentus</i> . . . . .	8
Figure 2.4	$^1\text{H}$ nuclear magnetic resonance spectroscopy (NMR) spectra of <i>C. crescentus</i> O-specific polysaccharide (OPS) . . . . .	9
Figure 2.5	Monosaccharide analysis of LPS . . . . .	10
Figure 2.6	The structure of the <i>C. crescentus</i> OPS. . . . .	11
Figure 2.7	2D NMR of <i>C. crescentus</i> polysaccharide (PS)1. . . . .	12
Figure 2.8	The structure of minor component, the end caps of the OPS. . . . .	13
Figure 2.9	The structure of the <i>C. crescentus</i> rhamnan. . . . .	14
Figure 2.10	The structure of the <i>C. crescentus</i> core oligosaccharide (OS). . . . .	15
Figure 2.11	Fragment of $^1\text{H}$ - $^{13}\text{C}$ heteronuclear single quantum coherence (HSQC) spectrum of the core. . . . .	16



# List of Abbreviations

## General abbreviations

ABC	ATP-binding cassette
<i>C. crescentus</i>	<i>Caulobacter crescentus</i>
COSY	Correlation spectroscopy
<i>E. coli</i>	<i>Escherichia coli</i>
EDTA	Ethylenediaminetetraacetic acid
EPS	Extracellular polysaccharide
ESI	Electrospray ionization
GC-MS	Gas chromatography-mass spectroscopy
gCOSY	Gradient correlation spectroscopy
gHMBC	Gradient heteronuclear multiple bond coherence
gHSQC	Gradient heteronuclear single quantum coherence
HMBC	Heteronuclear multiple bond coherence
HMQC	Heteronuclear multiple-quantum correlation spectroscopy
HSQC	Heteronuclear single quantum coherence
LPS	Lipopolysaccharide
MALDI-TOF	Matrix assisted laser desorption/ionization-time of flight mass spectroscopy
MS	Mass spectrometry
NMR	Nuclear magnetic resonance spectroscopy
NOE	Nuclear Overhauser enhancement
NOESY	Nuclear Overhauser enhancement spectroscopy
OPS	O-specific polysaccharide
OS	Oligosaccharide
PBS	Phosphate-buffered saline
PS	Polysaccharide
ROESY	Rotating frame nuclear Overhauser effect spectroscopy
S-layer	Protein surface layer
SDS-PAGE	Sodium dodecyl sulfate-polyacrylamide gel electrophoresis
TFA	Trifluoroacetic acid
TLC	Thin-layer chromatography
TCOSY	Total correlation spectroscopy
UV	Ultraviolet Light

## **Sugar abbreviations**

GalA	Galacturonic acid
Glc	Glucose
GlcA	Glucuronic acid
3-O-MeGlc	3-O-methylglucose
Hep	Heptose
Kdo	Ketodeoxyoctulosonic acid
Man	Mannose
PerN	Perosamine
Rha	Rhamnose

# **Acknowledgments**

Thank those people who helped you.

Don't forget your parents or loved ones.

You may wish to acknowledge your funding sources.

# Chapter 1

## Introduction

*But during the writing of this review, I learned how little I knew in this area, and this was a humbling and sobering experience. I am certain that I have made many mistakes due to my ignorance, and I hope that the review will be useful despite its many faults— Hiroshi Nikaido (2003), my grand supervisor.*

### 1.1 S-layer structure

Examples of bacteria with oblique S-layer are *Bacillus stearothermophilus* NRS2004/3a<sup>2</sup> and *Lactobacillus brevis*.<sup>3</sup> Examples of bacteria with rectangular S-layer are *Corynebacterium diphtheriae*<sup>4</sup> and *Aeromonas salmonicidae* A450.<sup>5</sup> An example of a bacterium with a triangular S-layer is *Sulfolobus acidocaldarius*.<sup>6,7</sup> Examples of bacteria with hexagonal S-layer are *Bacillus anthracis*<sup>8</sup> and *Caulobacter crescentus*.<sup>9</sup>

### 1.2 History of S-layers

---

<sup>2</sup>P. Messner, D. Pum, and U. B. Sleytr. *J Ultra Mol Struct Res*, **97**: 73–88, 1986.

<sup>3</sup>K. Masuda and T. Kawata. *Microb Immun*, **24**: 299–308, 1980.

<sup>4</sup>T. Kawata and K. Masuda. *Jpn J Microbiol*, **16**: 515–523, 1972.

<sup>5</sup>E. Ishiguro et al. *J Bacteriol*, **148**: 333–340, 1981.

<sup>6</sup>R. L. Weiss. *J Bacteriol*, **118**: 275–284, 1974.

<sup>7</sup>In:

<sup>8</sup>S. Holt and E. Leadbetter. *Bacteriol Rev*, **33**: 346–378, 1969.

<sup>9</sup>J Smit et al. *J Bacteriol*, **146**: 1135–1150, 1981.

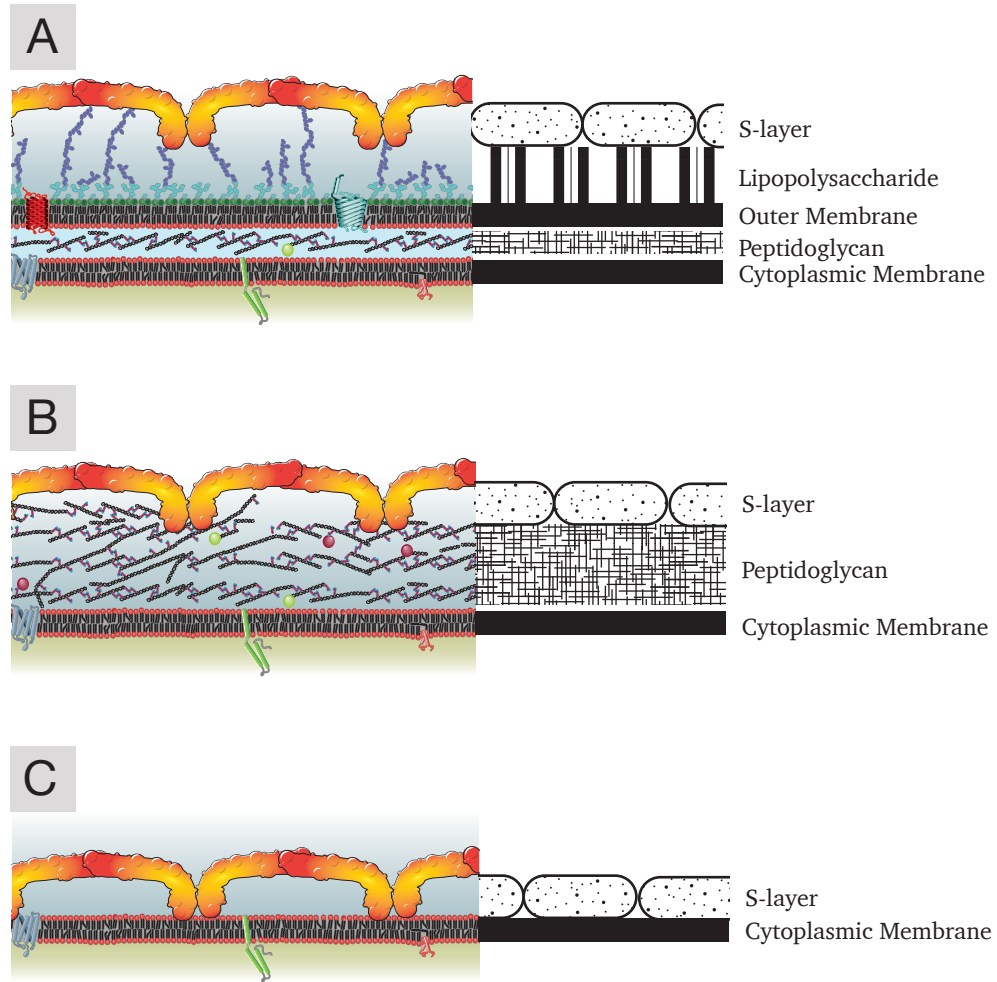


**Figure 1.1:** Cross-sectional diagrams of the cell envelopes of (A) Gram negative bacteria, (B) Gram positive bacteria, and (C) archaeabacteria. In all known cases the S-layer sits on the extreme outer surface of the cell. (This diagram was inspired by Fig. 1 from U. B. Sleytr and P. Messner. Crystalline surface layers on bacteria. *Annual Reviews in Microbiology*, **37**: 311–339, 1983.)

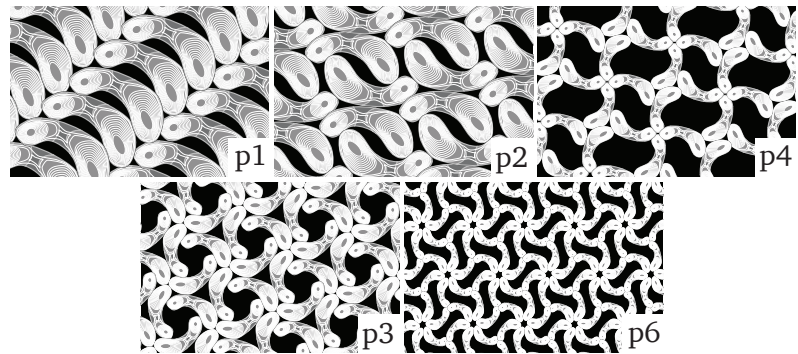


**Figure 1.2:** A simple overview of S-layer symmetries. p1 and p2 are oblique symmetries. p4 is a rectangular symmetry. p3 and p6 are triagonal/hexagonal symmetries.

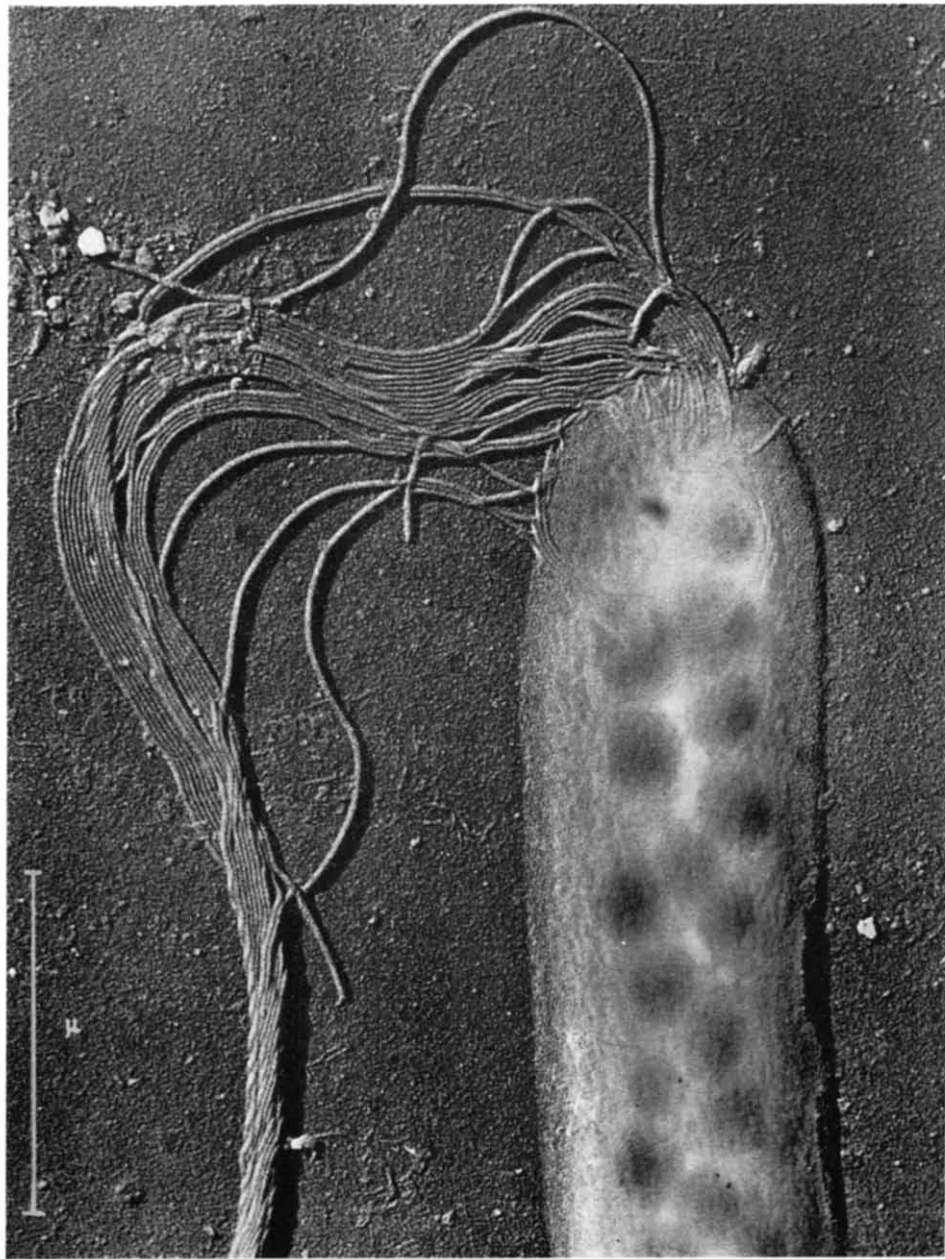


**Figure 1.3:** The first published image of a S-layer. The hexagonal S-layer on the surface of the bacterium — probably *Spirillum* sp. — is visible along the edges of the cell body (centre right). The scale bar denotes one micrometre. (This image is Fig. 1 from A. Houwink. A macromolecular mono-layer in the cell wall of *Spirillum* spec. *Biochimica et biophysica acta*, **10**: 360–366, 1953. reused with full permission from the publisher, Elsevier.)

# Chapter 2

## The core and O-polysaccharide structure of the *Caulobacter crescentus* lipopolysaccharide

“And so, progressively, the veil behind which Nature has so carefully concealed her secrets is being lifted where the carbohydrates are concerned.” — H. Emil Fischer, 1902 Nobel prize lecture  
My great-great-great-great-great-great-grand advisor.

### 2.1 Introduction

*Caulobacter crescentus* is an aquatic alphaproteobacterium well known for a stalked, crescent cell morphology, asymmetric cell division, and a protein surface layer (S-layer). *C. crescentus* is a widely studied model organism for cell development and differentiation; despite this, the structure of its lipopolysaccharide (LPS) has not previously been fully determined.

Interest in the LPS of *C. crescentus* is focused on its immunological profile<sup>11</sup> and its structural role as an anchor for the self-assembled, paracrystalline S-layer.<sup>12</sup> The LPS of *C. crescentus* possesses a much reduced immunogenic activity, most likely due to its lipid A structure, which is significantly different from that of LPS from enteric bacteria. The lipid A structure has been reported,<sup>11</sup> it is a unique molecule containing a di-diaminoglucose backbone (instead of di-glucosamine) and two galacturonate moieties that replace the canonical phosphates that are on each end of the disaccharide in most lipid A molecules. The *C. crescentus* S-layer non-covalently attaches to the O-specific polysaccharide (OPS).<sup>12</sup> However, the OPS structure has not been resolved. Genetic analyses have pointed towards the unusual N-acetylglucosamine being a major component.<sup>13</sup> A notable feature of this O-antigen is that it exists completely hidden beneath the S-layer, presumably inaccessible to the environment.<sup>12</sup> Carbohydrate structures from non-pathogenic bacterial LPS are rarely studied and an LPS that is sequestered beneath an S-layer is not represented in the literature.

<sup>11</sup>J. Smit et al. *Innate Immun*, **14**: 25–36, 2008.

<sup>12</sup>S. G. Walker et al. *J Bacteriol*, **176**: 6312–6323, 1994.

<sup>13</sup>P. Awram and J. Smit. *Microbiology*, **147**: 1451–1460, 2001.

In the present study our data has determined the core oligosaccharide (OS) structure from *C. crescentus* CB15 NA1000 (advancing an earlier report of core composition<sup>14</sup>), as well as the central backbone and non-reducing ends of its OPS. Unexpectedly, we identified a previously unknown rhamnan polysaccharide. Along with previous reports on lipid A<sup>11</sup> and extracellular polysaccharide (EPS),<sup>15</sup> we believe that all the major carbohydrate structures in *C. crescentus* cell envelope have now been solved.

## 2.2 Results

### 2.2.1 Characterisation of whole LPS

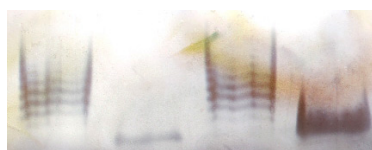


**Figure 2.1:** Visual comparison of silver stained *E. coli* O122 LPS and *C. crescentus* LPS. LPS samples were run on a SDS-PAGE and silver stained. Lanes 1 and 3 contain equal amounts of LPS from *E. coli* O122. Lanes 2 and 4 contain our isolated LPS from *C. crescentus*. Lane 4 has twice the loaded amount compared to lane 2 to demonstrate that there are no minor, hidden bands. Notice the canonical ‘laddering’ pattern of *E. coli* LPS and the distinctly singular band of *C. crescentus* LPS.

### 2.2.2 Initial assessment and component analysis

The polysaccharide (PS) was released from the LPS by hydrolysis with acetic acid. <sup>1</sup>H nuclear magnetic resonance spectroscopy (NMR) spectrum of the PS (fig. 2.4)) contained a large number of partially overlapping signals of various intensities in the anomeric region. It was obviously not a regular polymer with well-defined repeating units. Attempts to separate this material by anion-exchange chromatography led to the isolation of a number of fractions from neutral to slightly retained, but all of them had virtually identical NMR spectra. Methylation of the polysaccharide led to the identification of 3- and 3,4-substituted mannopyranose, terminal glucopyranose (derived from side-chain 3-O-MeGlc), terminal, 3-, 4-, and 2,4-substituted rhamnopyranose, 3-substituted PerNAc, and an unidentified derivative resembling methylated PerN that eluted between dimethylhexose derivatives and 3-substituted PerNAc. To identify the position of the methyl groups in naturally methylated monosaccharides, methylation was conducted with CD<sub>3</sub>I. This confirmed the identification of tetramethylglucitol as originating from 3-O-MeGlc, but did not identify any other naturally methylated monosaccharides, visible in NMR spectra. An unknown derivative received two deuterated methyl groups.

<sup>14</sup>N. Ravenscroft et al. *J Bacteriol*, **174**: 7595–7605, 1992.

<sup>15</sup>N. Ravenscroft et al. *J Bacteriol*, **173**: 5677–5684, 1991.

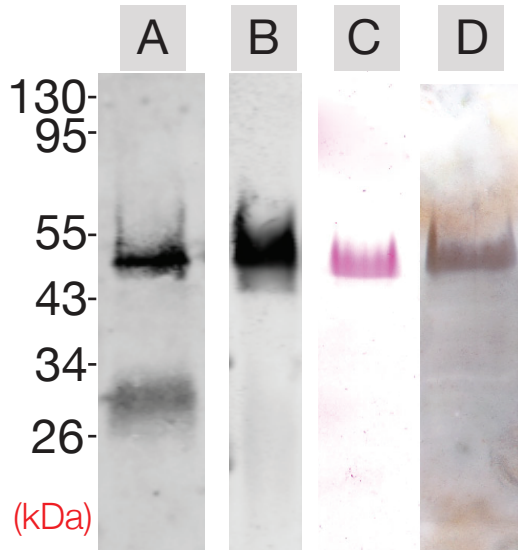


**Figure 2.2:** Four different visualisations of *C. crescentus* LPS. **A.** Western blot with rabbit anti-OPS serum used as the primary probe. **B.** Far-western blot with RsaA Δ277-784 used as the primary probe and rabbit anti-RsaA serum used as the secondary probe. **C.** Schiff stained SDS-PAGE. **D.** Silver stained SDS-PAGE. The smooth-LPS (*i.e.* containing a complete OPS) runs as a single band at roughly the equivalent rate of a 50 kDa protein and is visible in all lanes. The faint band visible at 30 kDa in the western blot (A) is of unknown source. The faint 30 kDa band is not seen in by far western (B), Schiff stain (C), or silver stain (D).

### 2.2.3 O-antigen structure determination (PS1)

A set of 2D spectra [gradient correlation spectroscopy (gCOSY), total correlation spectroscopy (TCOSY), nuclear Overhauser enhancement spectroscopy (NOESY),  $^1\text{H}$ - $^{13}\text{C}$  gradient heteronuclear single quantum coherence (gHSQC), gradient heteronuclear multiple bond coherence (gHMBC)] was obtained for the PS. There were many (more than 20) lines of correlations from the anomeric signals. Later, after the analysis of PS degradation products, most of them could be assigned to particular structures (figs. 2.6, 2.8, and 2.9). Polysaccharide heterogeneity was not caused by random acetylation, but PS contained 4 methyl groups (one major and 3 minor). Monosaccharide analysis revealed L-Rha, D-Man, D-PerN (perosamine, 4-aminodeoxyrhamnose), and 3-O-MeGlc. Other methylated monosaccharides were not identified by gas chromatography-mass spectroscopy (GC-MS) as alditol acetates, possibly due to low content or degradation during hydrolysis. The GC-MS data is presented in fig. 2.5.

In an attempt to simplify the structure, PS was oxidized with  $\text{NaIO}_4$ , reduced with  $\text{NaBD}_4$ , hydrolysed with 2% AcOH, and the products were separated on a Biogel P6 column to give a polymer and an OS, OS1. Analysis of OS1 will be described below. For some reason not all of the rhamnan was oxidized, and some of its signals persisted in the spectra of the remaining polymer (without side-chain Rha F). To remove the rest of it, the oxidation was repeated to produce PS1. Spectra still contained some signals of minor components, analysed later. Assignment of the spectra of the non-oxidisable polymer PS1 was difficult due to complete

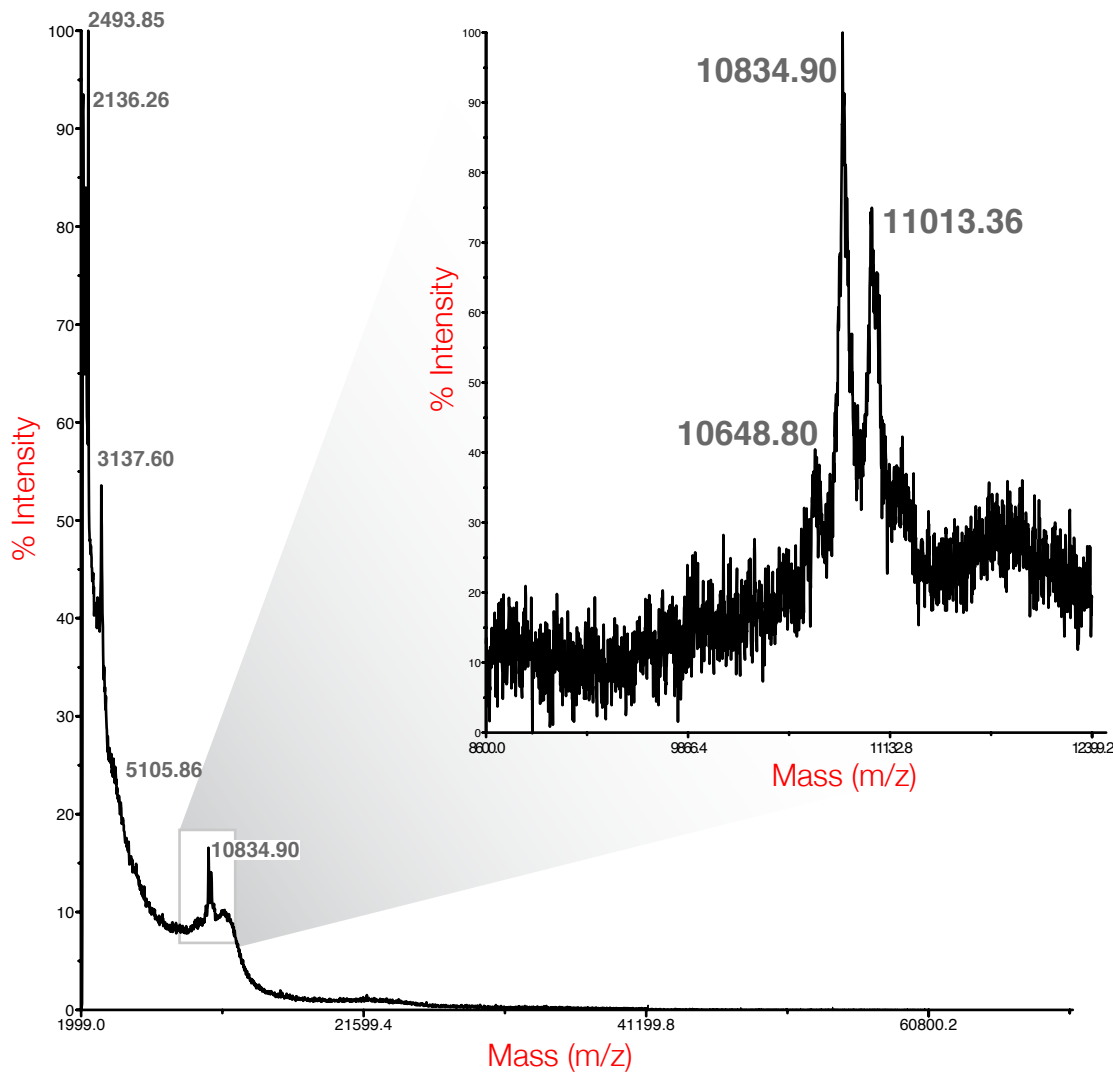


**Figure 2.3:** MALDI-TOF analysis of intact, whole LPS from *C. crescentus*. The insert highlights the peaks attributed to LPS. The major LPS peak is labelled 10834.90 m/z

or partial overlap of the H-2,3,4,5 signals of PerNAc. To improve signal spread, PS1 was deacylated with 4 M NaOH. At this point the major polymer became positively charged and an attempt was made to separate it from the minor components using cation-exchange chromatography. However, all material was eluted together at high salt concentration, thus indicating that all components were chemically bound together. Assignment of the spectra (fig. 2.7, table 2.1) became possible at this stage due to better signal spread (H-4 signals of PerN moved to high field due to deacylation) and the sequence shown on fig. 2.6 was proposed. Spectra contained the signals of two  $\beta$ -mannopyranose,  $\alpha$ -3-O-MeGlc, and two -Per4N. The following interresidual nuclear Overhauser enhancement (NOE) and heteronuclear multiple bond coherence (HMBC) correlations were used to determine the sequence: R1:L3, L1:Z3, Z1:Q3, Q1:W3, W1:X3, A1:X4. PS1 had trisaccharide repeating units composed of  $\beta$ -mannose and two  $\alpha$ -PerNAc residues, and every second repeating unit carried a side branch of 3-O-MeGlc. It seems that side-chains were present quite regularly at

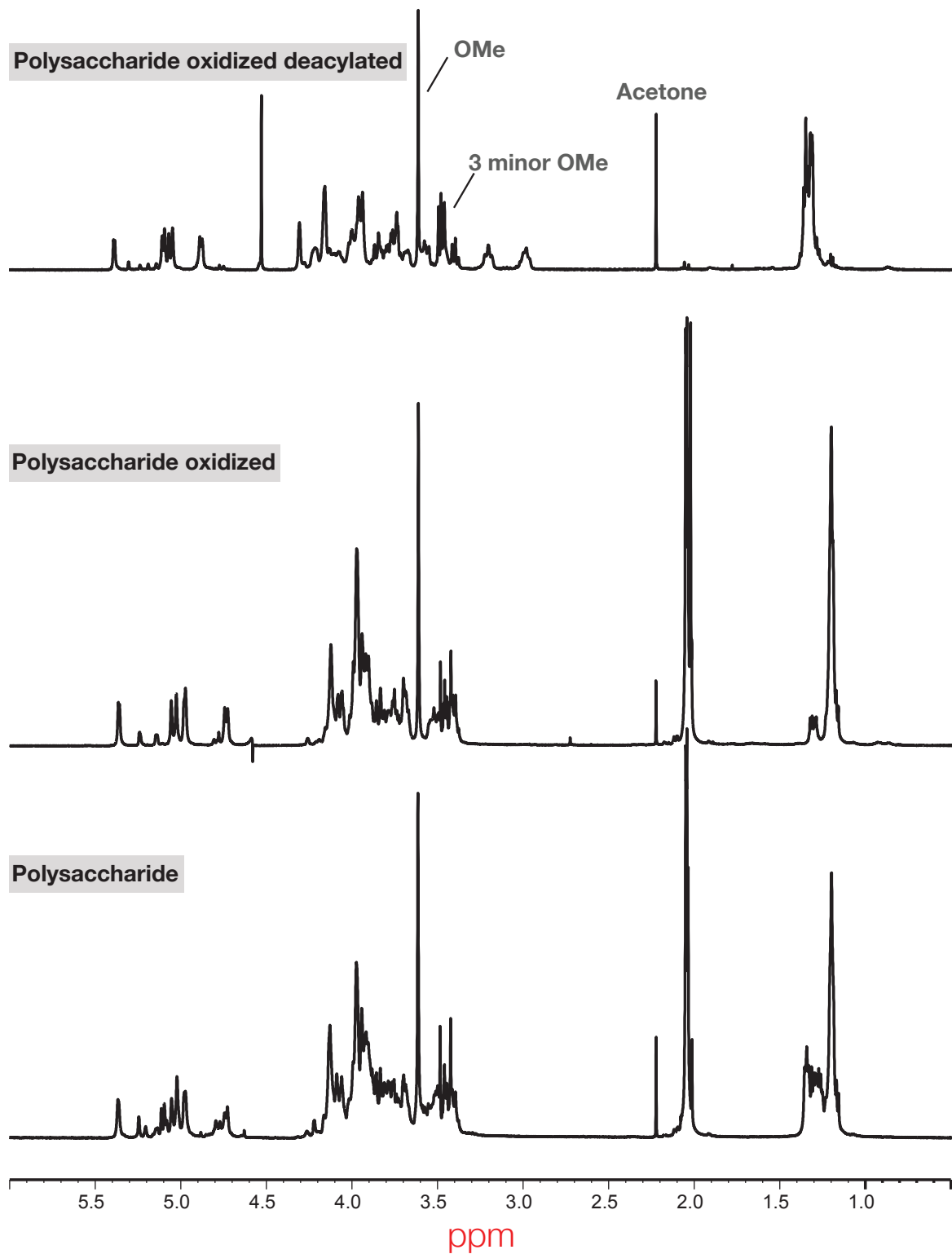


**Figure 2.4:**  $^1\text{H}$  NMR spectra of the intact *C. crescentus* OPS (bottom trace), double oxidized polysaccharide (middle trace) and N-deacylated double oxidized polysaccharide (upper trace).

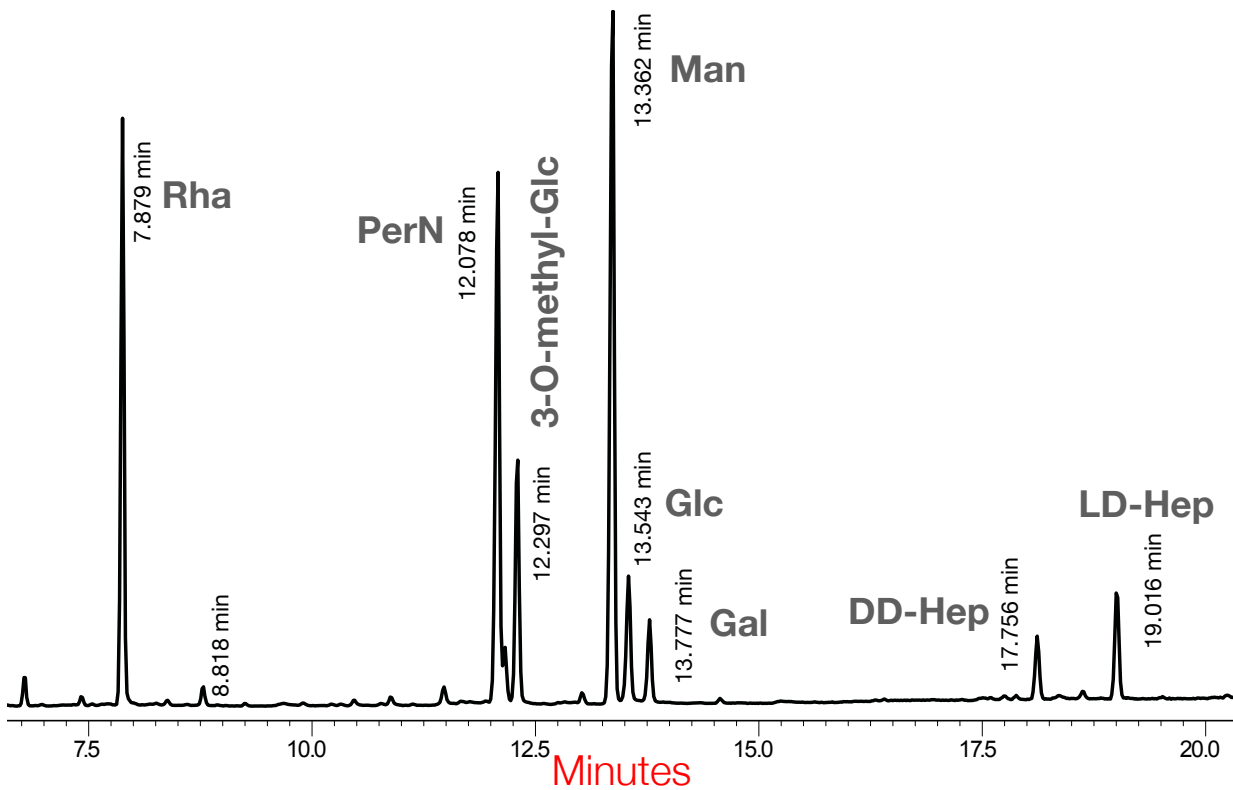
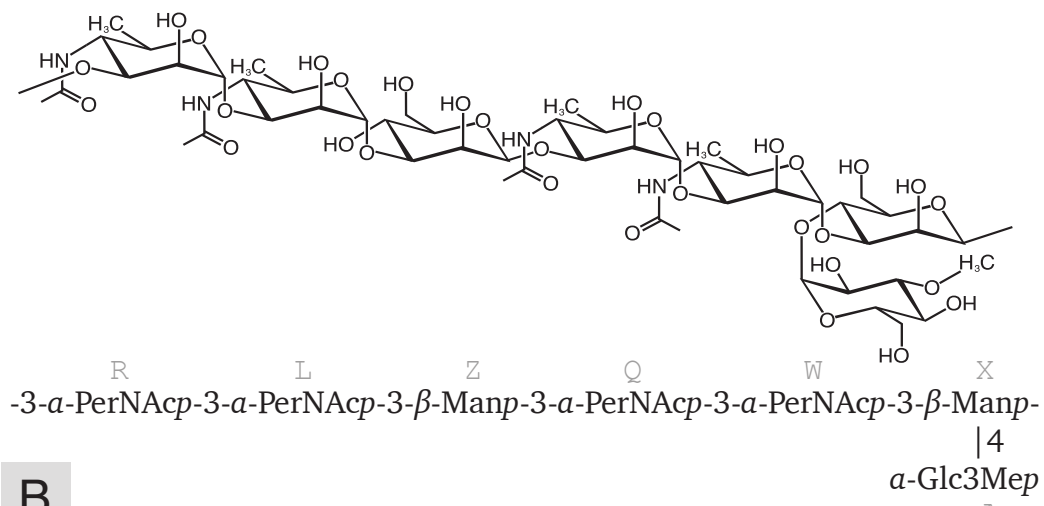


**Figure 2.5:** Monosaccharide analysis of *C. crescentus* LPS. Alditol acetates derivatives of the LPS component monosaccharides were separated and identified by GC-MS. The protocol used is described on page 18.

each second trisaccharide repeat of the main chain, because NOE correlations were observed between the repeating units with and without 3-O-MeGlc, and not between units of the same structure. Thus altogether, the repeating unit contained seven monosaccharides.

**A**



**B**

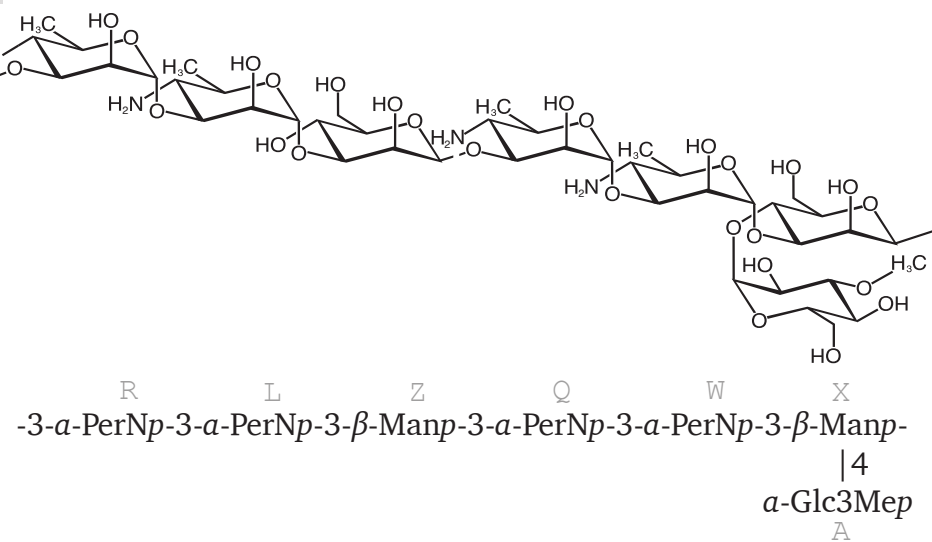


**Figure 2.6:** The structure of the *C. crescentus* OPS. **A.** The intact repeating unit, PS1. **B.** The deacetylated product of PS1.

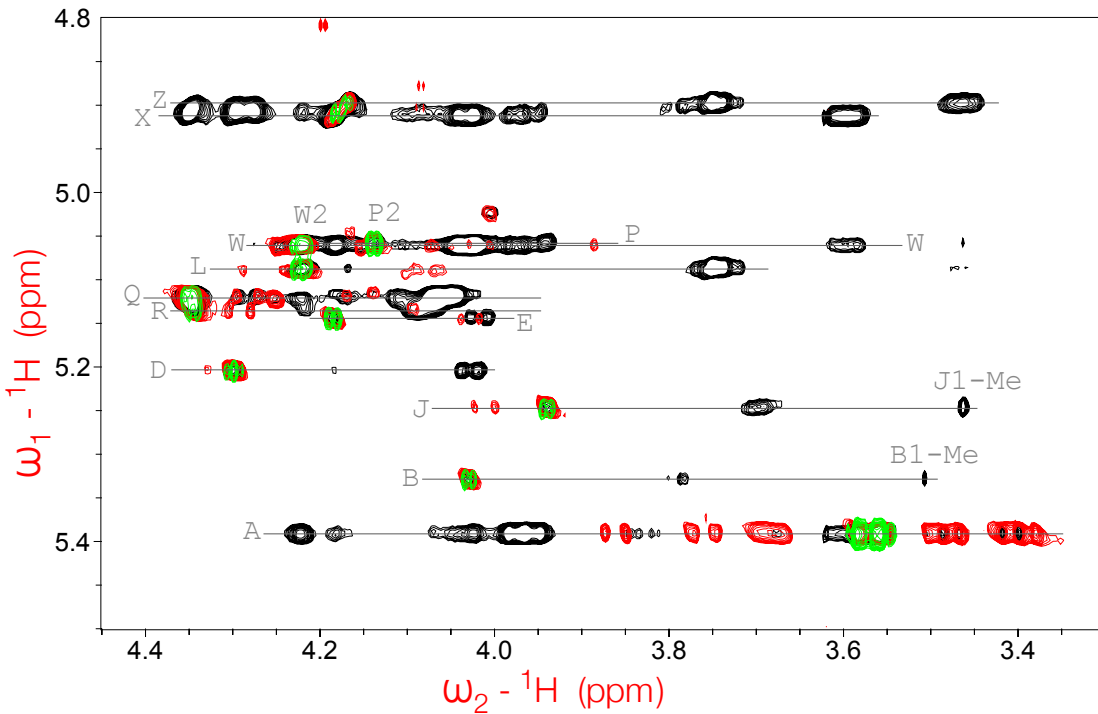


**Figure 2.7:** Overlap of COSY (green), TCOSY (red) and ROESY (black) correlations from anomeric protons of double oxidized deacylated *C. crescentus* PS1.

#### 2.2.4 Minor component determination

PS and PS1 spectra contained signals of minor components, which could not be removed by chromatography, as described above. They probably represented the non-reducing ends of the major chain, PS1 (fig. 2.8). The minor components contained methylated Rha (2-O-Me-Rha residue J and 2,3-Me<sub>2</sub>-PerN residue B). The position of the methyl groups were found from HMBC correlations between protons of methyl groups and carbon atoms bearing OMe groups, which all were well visible and did not overlap with other signals due to their low field position. Thus, two independent structural fragments, 1 and 2, were found and are shown in fig. 2.8. Mannose residues Z' and Z'' at the non-reducing ends of these fragments were further linked to PerN residues, indistinguishable from the PerN of the main chain. PerN residue D had upfield shifted C-2 and downfield shifted C-3 signals (table 2.2)), which have not been explained. It appears that its O-3 was phosphorylated, producing typical phosphorylation signal shifts and broadening of the H-3 signal, but <sup>1</sup>H-<sup>31</sup>P heteronuclear multiple-quantum correlation spectroscopy (HMQC) NMR spectrum showed no signals, possibly due to the low abundance of this residue. Possibly Rha residues inserted in the structure resembling PS1 represented the attachment point of the rhamnan (PS2) to PS1, if they were linked together.

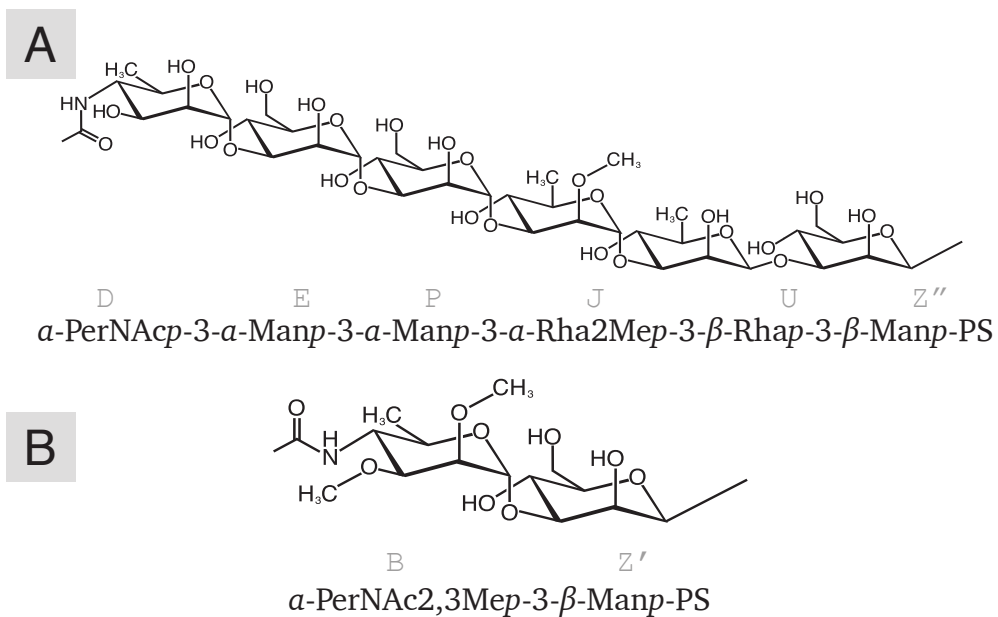


**Figure 2.8:** The structure of minor component, the end caps of the OPS. **A.** Fragment 1. **B.** Fragment 2.

### 2.2.5 Rhamnan polysaccharide determination (PS2)

Periodate oxidation of the PS produced an OS1, which was analyzed by NMR and its structure, as shown on fig. 2.9, was determined using standard 2D NMR methods. Signal assignment is shown in the table 2.3. It contained three rhamnopyranose units and 4-deoxy-1-deutero-erythritol, produced by the oxidation-reduction of 4-substituted rhamnose. Formation of this oligosaccharide could be explained by oxidation of the side chain Rha F and 4-substituted Rha G in the PS1 (letter labels for monosaccharides were given using anomeric signals in the whole PS spectra starting from low-field). The unoxidized 4-substituted residue T in the oligosaccharide originally carried side-chain Rha F at position 2. Knowing the OS1 structure the signals of a corresponding polymer (PS2) were identified in the spectra of the whole PS, and are given in the table 2.3.

### 2.2.6 Core oligosaccharide determination

The core oligosaccharide of the *C. crescentus* LPS isolated after AcOH hydrolysis contained one non-degraded Kdo, two LD-Hep, one DD-Hep, mannose, galactose, and glucuronic acid in pyranose form. 2D NMR analysis led to the structure shown on fig. 2.10 (NMR assignments are in table 2.4, the heteronuclear single quantum coherence (HSQC) spectrum is in fig. 2.11). The sequence followed from the observed NOE: E1:C5,C7,F5; F1:E2; G1:F3; H1:C7,E2; K1:C4; L1:K4. Correlation E1:C7 is always observed in the  $\alpha$ -Hep-5-Kdo fragment. E1:F5 was due to the  $\alpha$ -Man-2-Hep linkage. H1E2 indicates spatial proximity of the residues E and H, linked to the same Kdo C. All expected transglycoside correlations were observed in HMBC spectrum, together with intra-ring correlations H-1:C-3 and H-1:C-5 for all  $\alpha$ -pyranoses.

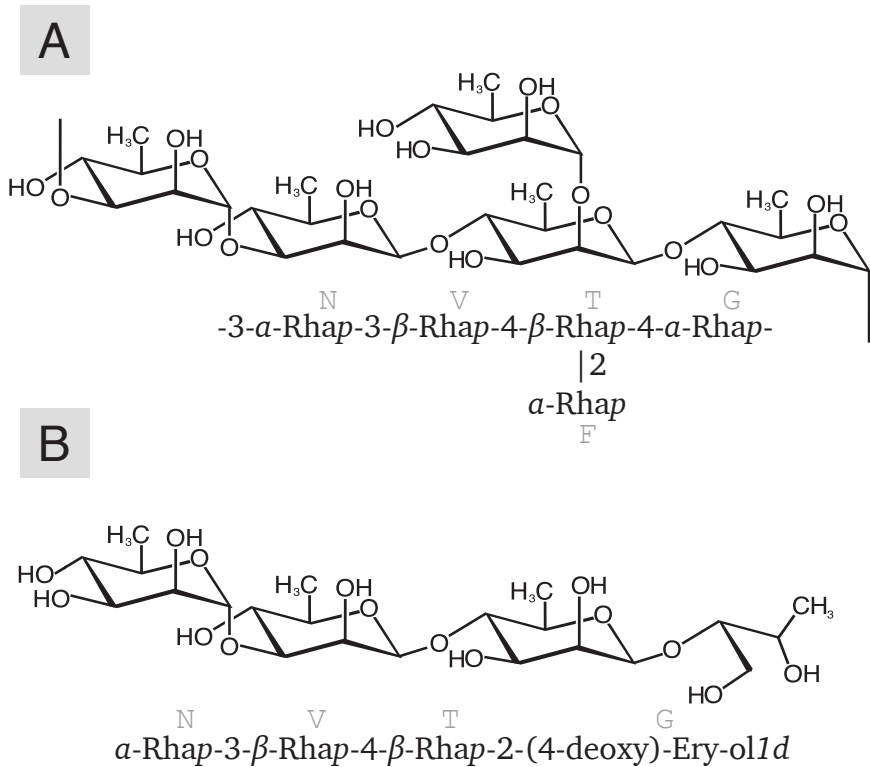


**Figure 2.9:** The structure of the *C. crescentus* rhamnan. **A.** the intact rhamnan, PS2. **B.** the oxidised rhamnan product, OS1.

Methylation analysis revealed terminal DD-Hep, terminal and 2-substituted LD-Hep, 3-substituted Man and terminal Gal. The structure agreed with mass spectral data, electrospray ionization (ESI) mass spectrometry (MS) in negative ion mode,  $[M-H]^- = 1314.9$ ,  $[M-2H]/2^- = 656.7$ , calculated exact mass Hex x 2 + Hep x 3 + HexA x 1 + Kdo x 1 = 1314.4 Da.

## 2.3 Methods

### 2.3.1 Bacterial strain construction and growth conditions

The strain used for the preparation of LPS was JS1025, a derivative of *C. crescentus* CB15 NA1000. The salient features are that it has an engineered amber mutation in *rsaA* leading to the loss of the S-layer and the gene CCNA\_00471 has been inactivated by a partial deletion. CCNA\_00471 encodes a putative GDP-L-fucose synthase.<sup>16</sup> The knockout ( $\Delta 471$ ) confers a deficiency in an EPS that was previously found to contain L-fucose.<sup>15</sup> CCNA\_00471 was disrupted in the same manner as previously in JS4038,<sup>17</sup> except the starting strain used here was JS1023.<sup>18</sup>

<sup>16</sup>M. E. Marks et al. *J Bacteriol*, **192**: 3678–3688, 2010.

<sup>17</sup>C. Farr et al. *PLoS One*, **8**: e65965, 2013.

<sup>18</sup>F. Amat et al. *J Bacteriol*, **192**: 5855–5865, 2010.

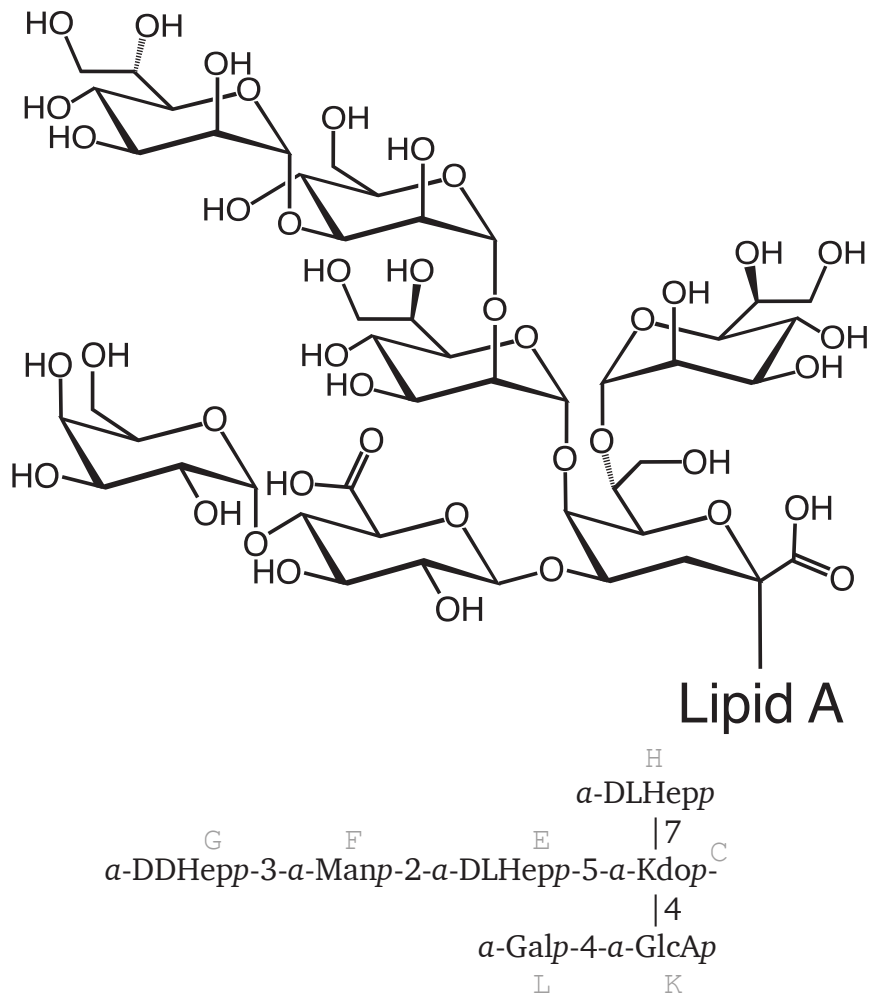


**Figure 2.10:** The structure of the *C. crescentus* core OS.

Cells were grown to mid-to-late log phase ( $OD_{600} = 0.9$ ) in M16HIGG defined medium at 30°C in 2.8 1 Fernbach flasks containing 1250 ml of medium, shaking at 100 rpm. M16HIGG is a modification of M6HIGG medium,<sup>19</sup> containing 0.31% glucose, 0.09% glutamate, 1.25 mm sodium phosphate, 3.1 mm imidazole, 0.05% ammonium chloride and 0.5% modified Hutner's Mineral Base.<sup>20</sup>

### 2.3.2 LPS isolation

LPS was isolated from the cells via disrupting the outer membrane by chelation. The negative charges in Gram negative bacterial LPS are stabilised and bridged by available divalent cations (*i.e.*  $Ca^{2+}$  and  $Mg^{2+}$ ). Lieve first noted in 1965<sup>21</sup> that one can strip the counter ions from the outer membrane to disrupt it and cause it to shed into the medium. We chose a chelation strategy because we found it easy to scale

<sup>19</sup>J. Smit, M. Hermodson, and N. Agabian. *J Biol Chem*, **256**: 3092–3097, 1981.

<sup>20</sup>G. CohenBazire, W. Sistrom, and R. Stanier. *J Cell Comp Physiol*, **49**: 25–68, 1957.

<sup>21</sup>L. Leive. *Biochem Biophys Res Commun*, **21**: 290–296, 1965.

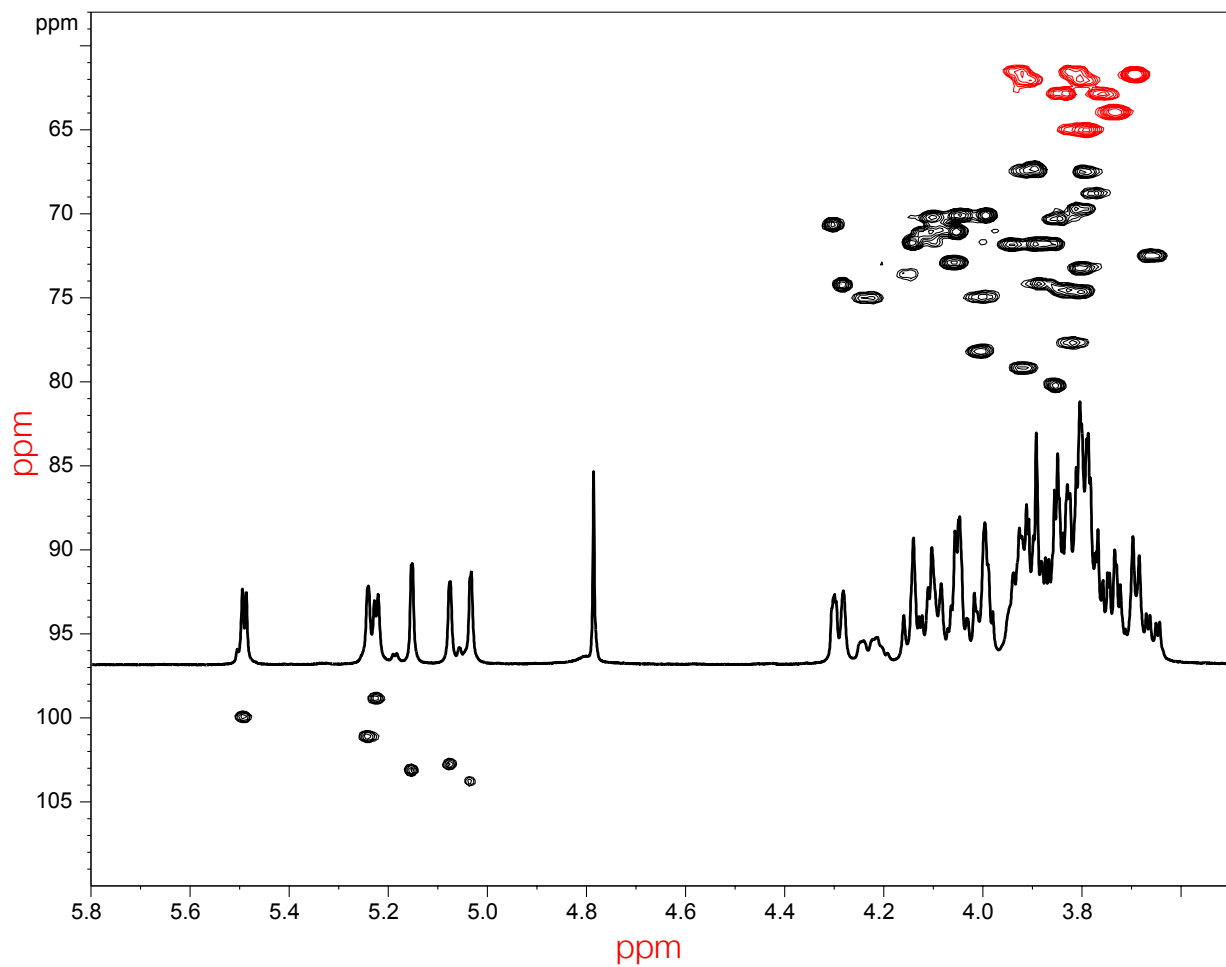


**Figure 2.11:** Fragment of  $^1\text{H}$ - $^{13}\text{C}$  HSQC spectrum of the core.

up, it didn't require noxious organic solvents, and because our lab's first attempt to isolate and analyse *C. crescentus* LPS<sup>14</sup> using the Darveau extraction method<sup>22</sup> only resulted in the isolation of core+lipidA (rough LPS).

The protocol we used was a modification of the procedure reported by Walker et al.<sup>12</sup> Cells were centrifuged at 12 400 x g for 10 min. The pellets were suspended with distilled water and re-centrifuged. These pellets were resuspended in 1/10 original culture volume in phosphate-buffered saline (PBS)<sup>23</sup> amended with 35 mM ethylenediaminetetraacetic acid (EDTA), agitated at room temperature for 10 min and then centrifuged at 15 300 x g for 15 min. The supernatant was retrieved and re-centrifuged, as before, to ensure clarity and then dialysed against 5 mM MgCl<sub>2</sub>. DNase and RNase were added to final concentrations of 10 µg ml<sup>-1</sup> and 100 µg ml<sup>-1</sup>, respectively, and incubated at 37°C for 2 h. Proteinase K was added to a final concentration of 0.3 mg ml<sup>-1</sup> and the preparation was incubated at 50°C overnight. The sample was then ultracentrifuged at 184 000 x g for 3 h. Glassy pellets formed which were suspended in distilled water

<sup>22</sup>R. P. Darveau and R. E. Hancock. *J Bacteriol*, **155**: 831–838, 1983.

<sup>23</sup>T. Maniatis, E. F. Fritsch, and J. Sambrook. *Molecular cloning: a laboratory manual*. vol. 545 Cold Spring Harbor, NY, 1982.

to 1/100 original culture volume. A Bligh-Dyer extraction was performed to reduce contaminating lipids.<sup>24</sup>

### 2.3.3 Bligh Dyer Extraction

A Bligh Dyer extraction was performed on all LPS preparations to reduce the presence of contaminating lipids. The extraction was performed as first published.<sup>24</sup> In short, to one volume of aqueous LPS sample, 3.75 volumes of chloroform/methanol (1:2 v/v) was added and the sample was vortexed for 30 seconds. 1.25 volumes of chloroform was added and the sample was vortexed again for 30 seconds. 1.25 volumes of water were added and the sample was vortexed a final time for 30 seconds. This mixture was then centrifuged at 15 300 x g for 10 min. After centrifugation, the mixture separated into two phases, a lower organic phase and an upper aqueous phase. The LPS partitions into the aqueous phase, while other lipids partition into the organic phase. The aqueous phase was retrieved and kept.

### 2.3.4 Gel electrophoresis

Discontinuous SDS-PAGE was performed with a 13% separating gel.<sup>25</sup> Detection of LPS was done by periodate oxidation and silver staining as described by Zhu et al.<sup>26</sup>

### 2.3.5 NMR spectroscopy

NMR experiments were carried out on a Varian INOVA 600 MHz (<sup>1</sup>H) spectrometer with 5 mm gradient probe at 25–50°C with acetone internal reference (2.225 ppm for <sup>1</sup>H and 31.45 ppm for <sup>13</sup>C), using standard pulse sequences gCOSY, TCOSY(mixing time 120 ms), ROESY (mixing time 300 ms), gHSQC, and gHMBC(100 ms long range transfer delay), HMQC for <sup>1</sup>H-<sup>31</sup>P correlation, J<sub>HX</sub> set to 10 Hz. Acquisition time was kept at 0.8–1 sec for H-H correlations and 0.25 sec for HSQC. 256 increments were acquired for t<sub>1</sub> in all 2D spectra, except 512 for gCOSY.

### 2.3.6 LPS Chromatography

Gel chromatography was performed on a Sephadex G-15 column (1.5 x 60 cm) or a Bio-gel P6 column (2.5 x 60 cm) in pyridine-acetic acid buffer (4 ml:10 ml:1 l water), and monitored by refractive index detector (Gilson). Anion exchange chromatography was done on an Hitrap Q column (2x5 ml size, Amersham), with ultraviolet Light (UV) monitoring at 220 nm in a linear gradient of NaCl (0–1 M, 1 h) at the 3 ml min<sup>-1</sup>. Fractions of 1 min were collected and additionally tested for carbohydrates, by spotting on an SiO<sub>2</sub> thin-layer chromatography (TLC) plate, dipping them in 5% H<sub>2</sub>SO<sub>4</sub> in EtOH and heating with a heat-gun. All fractions of interest were dried in a Savant drying centrifuge and <sup>1</sup>H spectra were recorded for each fraction without desalting. For 2D NMR, desalting was performed on a Sephadex G15 column.

<sup>24</sup>E. G. Bligh and W. J. Dyer. *Can J Biochem Physiol*, **37**: 911–917, 1959.

<sup>25</sup>U. K. Laemmli. *Nature*, **227**: 680–685, 1970.

<sup>26</sup>Z.-X. Zhu et al. *Electrophoresis*, **33**: 1220–1223, 2012.

### **2.3.7 Monosaccharide analysis**

Samples with added inositol standard were hydrolysed with 3 M trifluoroacetic acid (TFA) at 120°C. Monosaccharides were converted to alditol acetates by conventional methods and identified by GC-MS on a Varian Saturn 2000 instrument on a DB17 capillary column (30 m x 0.25 mm ID x 0.25 µm film) with helium carrier gas, using a temperature gradient 170°C (3 min)–250°C at 5°C min<sup>-1</sup>.

### **2.3.8 Determination of absolute configurations of monosaccharides**

To the polysaccharide sample (0.2 mg) (R)-2-BuOH (0.2 ml) and acetyl chloride (0.02 ml) were added at room temperature, heated at 90°C for 2 h, dried by air stream, acetylated, analysed by GC-MS as described above. Standards were prepared from monosaccharides of known configuration with (R)- and (S)-2-BuOH.

### **2.3.9 Methylation analysis**

For the methylation analysis core sample (2 mg) was dephosphorylated with 50 µl of 48% HF for 20 h at +10°C, diluted with 2 ml of ethanol, precipitate collected by centrifugation, washed with 2 ml of ethanol, dried.

Methylation was performed by Ciucanu-Kerek procedure.<sup>27</sup> 0.5 mg of the sample was dissolved in 0.5 ml of dry DMSO with heating at 100°C for 5–10 min until complete dissolution. Powdered NaOH (about 50 mg) was added and the mixture was stirred for 30 min. 0.2 ml of MeI was added and the mixture was stirred for a subsequent 30 min. The sample was then flushed with air to remove the MeI and diluted to 10 ml with water. The sample was passed through a C18 Seppak cartridge, washed with 10 ml of water, and then the methylated compound was eluted with 5 ml of methanol. The methylated product was hydrolysed with 3 M TFA (120°C, 3 h), dried, reduced with NaBD<sub>4</sub>, and the reagent destroyed with 0.5 ml of 4 M HCl. The solution was dried under a stream of air and dried twice more with the addition of MeOH (1 ml). The sample was acetylated with 0.4 ml Ac<sub>2</sub>O and 0.4 ml pyridine for 30 min at 100°C. It was then dried and analysed by GC-MS.

### **2.3.10 Periodate oxidation**

PS (10 mg) was dissolved in water (2 ml). NaIO<sub>4</sub> (20 mg) was added and the solution was incubated at room temperature for 24 h. Ethylene glycol (0.2 ml) and an excess NaBD<sub>4</sub> were added. The solution was then kept for 1 h before being treated with 0.2 ml of AcOH and desalted on a Sephadex G-15 column. The product was hydrolysed with 2% AcOH, 2 h at 100°C, and separated on a Sephadex G-50 column to give os1.

---

<sup>27</sup>I. Ciucanu and F. Kerek. *Carbohydr Res*, **131**: 209–217, 1984.

## 2.4 Discussion

The LPS of *C. crescentus* has an unusually complicated structure with two different polysaccharides, irregular substituents, and unfavourable NMR spectra. Presented data show structures of the core part, two polymers, and putative terminal structures. The polysaccharides could not be separated by size exclusion or anion-exchange chromatography and are probably linked together through the same core. The core of the *C. crescentus* LPS has been studied previously and an initial assessment of its composition was made,<sup>14</sup> but the complete structure had not been determined. The structure of the OPS has not been studied before. In our view the polysaccharide structure of the *C. crescentus* LPS represents one of the most complicated bacterial LPS polysaccharide structures identified so far.

The Kdo present in the LPS core structure (see fig. 2.10) has the typical substitutions at O-4 and O-5 of a manno-configured sugar and a negatively charged sugar, respectively.<sup>28</sup> It also has a rarely observed third substitution at O-7 with a heptose moiety. The Kdo O-7 position is known to be occupied by a galactose moiety in the core of *Rhizobium leguminosarum* bv. *Viciae* VF39,<sup>29</sup> and the secondary Kdo in the core oligosaccharide from *Acinetobacter baumannii* ATCC 19606 has an O-7 substituted with a glucosamine.<sup>30</sup>

In the traditional model LPS occupies the outer leaflet of the outer membrane of a Gram-negative bacterium, and so (excepting the presence of cell associated EPS) is the outermost layer of the cell. For *C. crescentus*, however, LPS is the penultimate barrier below the protein S-layer. The *C. crescentus* OPS serves as the anchor for the S-layer and is likely not accessible to the environment.<sup>12</sup> The carbohydrates found in the OPS are particularly hydrophobic, marked by the abundance of deoxy-sugars, acetyl groups, and methyl groups. This hydrophobicity is possibly a result of particular sugars needed for S-layer anchoring, as these carbohydrate structures likely evolved as the cognate ligands for the S-layer protein, RsaA. The distance between the S-layer and the outer membrane is about 17–19 nm.<sup>31</sup> It is possible the hydrophobicity aids in packing the polysaccharides between the S-layer and the LPS. Further determination of RsaA's structure should help illuminate the interaction between the S-layer and OPS.

Knowledge of the structure of *C. crescentus* OPS and LPS will facilitate the determination and characterization of their biosynthetic enzymes and mutant variants. Already, the enzymes LpxI<sup>32</sup> and GDP-L-perosamine acetylase<sup>33</sup> from *C. crescentus* have been characterized. One uncharacterised enzyme, WbqL, is necessary for proper OPS synthesis and disruption of wbqL leads to the accumulation of truncated and S-layer anchoring deficient OPS in the inner membrane and inhibits Crescentin-mediated cell curvature.<sup>34</sup> Many genes, such as wbqL, have been identified as essential for OPS synthesis<sup>13</sup> but have not yet been characterized. Other genes, that must be essential for OPS synthesis, have yet to be identified or characterized, such as the O-antigen polymerase and ligase.

The subunit-based repeating nature of *C. crescentus* OPS suggests that a Wzy-dependent pathway

<sup>28</sup>H. Brade. *Endotoxin in health and disease*. New York: Marcel Dekker, 1999. xviii, 950 p.

<sup>29</sup>Y. Zhang, R. I. Hollingsworth, and U. B. Priefer. *Carbohydr Res*, **231**: 261–271, 1992.

<sup>30</sup>E. V. Vinogradov et al. *Eur J Biochem*, **243**: 122–127, 1997.

<sup>31</sup>A. Moll et al. *Mol Microbiol*, **77**: 90–107, 2010.

<sup>32</sup>L. E. Metzger IV et al. *Nat Struct Mol Biol*, **19**: 1132–1138, 2012.

<sup>33</sup>J. B. Thoden et al. *Biochemistry*, **51**: 3433–3444, 2012.

<sup>34</sup>M. T. Cabeen et al. *J Bacteriol*, **192**: 3368–3378, 2010.

synthesizes the polymer.<sup>35</sup> The previous study that aimed to identify genes essential for OPS did not identify many of the canonical genes in the Wzy-dependant pathway,<sup>13</sup> such as the O-unit transporter, Wzx, O-antigen polymerase, Wzy; the chain-length determinate protein, Wzz; and the O-antigen ligase, WaaL. Genes that have been annotated as putative O-antigen synthesis genes do appear in the sequenced genomes for *C. crescentus* CB15, but they have not been experimentally confirmed.

An additional aspect to this LPS is the fact that its O-antigen is of homogeneous length. While other LPSS vary in size due to the number of O-antigen repeat groups, appearing as a laddering of bands by SDS-PAGE, the LPS from *C. crescentus* appears as a single band.<sup>12</sup> Initial MALDI-TOF analysis of the entire LPS indicates a size of about 10.8 kDa (see fig. 2.3 on page 8). After accounting for the solved structures for the lipid A and core regions, this suggests the LPS contains approximately 5 repeats of the proposed heptameric O-antigen structure. There is not currently a known mechanism for the regulation and synthesis of a strictly homogeneous length O-antigen. It is possible that this OPS is synthesized via the ATP-binding cassette (ABC)-transporter-dependent pathway<sup>35</sup> or another heretofore undiscovered mechanism. In any event it would seem that the transfer of a polysaccharide of this considerable size to the outer leaflet of the outer membrane is a remarkable feat for the bacterium.

---

<sup>35</sup>C. R. H. Raetz and C. Whitfield. *Annu Rev Biochem*, **71**: 635–700, 2002.

**Table 2.1:** NMR data for *C. crescentus* PS1 (40°C) and deacylated PS1 (50°C). Me at 3.62/61.3 ppm.

		PS1					
		1	2	3	4	5	6
PerNAc R	H	4.97	3.98	4.13	3.92	3.91	1.21
	C	103.3	68.2	75.5	52.4	69.4	18.0
PerNAc Q	H	4.98	3.97	4.11	3.92	3.91	1.21
	C	103.3	68.2	75.5	52.4	69.4	18.0
PerNAc L	H	5.05	4.12	3.99	3.98	3.98	1.21
	C	103.3	70.4	78.2	53.0	69.4	18.0
PerNAc W	H	5.02	4.12	3.96	3.98	3.98	1.21
	C	104.0	70.4	77.8	53.0	69.4	18.0
$\beta$ -Man X	H	4.74	4.09	3.98	3.90	3.54	3.80; 3.96
	C	97.8	72.1	85.4	72.1	75.8	62.6
$\beta$ -Man Z	H	4.72	4.06	3.70	3.68	3.41	3.77; 3.96
	C	98.2	71.9	82.3	67.2	77.3	62.4
Glc3Me A	H	5.36	3.51	3.40	3.44	3.68	3.75; 3.85
	C	100.0	72.2	84.1	70.1	74.1	61.6
Deacylated PS1							
PerN R	H	5.13	4.34	4.29	3.30	4.18	1.38
	C	103.5	67.4	75.0	53.4	67.8	18.0
PerN Q	H	5.11	4.34	4.29	3.30	4.18	1.38
	C	103.5	67.4	75.0	53.4	67.8	18.0
PerN L	H	5.08	4.22	4.06	3.11	4.09	1.35
	C	103.9	69.9	79.9	53.6	69.5	18.0
PerN W	H	5.06	4.22	4.06	3.11	4.09	1.35
	C	103.9	69.9	79.9	53.6	69.5	18.0
$\beta$ -Man X	H	4.91	4.18	4.03	3.96	3.59	3.83; 3.96
	C	98.0	71.7	85.0	71.7	75.9	62.1
$\beta$ -Man Z	H	4.90	4.18	3.75	3.75	3.46	3.83; 3.96
	C	98.0	71.7	82.0	67.0	77.4	62.1
Glc3Me A	H	5.39	3.57	3.40	3.48	3.68	3.76; 3.86
	C	100.2	72.2	84.0	70.0	74.1	61.7

**Table 2.2:** NMR data for the minor components of the double oxidized non-deacylated PS (50°C).  
Methyl group signals: B2: 3.48/59.5; B3: 3.42/57.9; J2: 3.45/59.6 ppm (H/C)

		1	2	3	4	5	6
PerN2,3Me B	H	5.25	3.96	3.71	3.81	3.91	1.17
	C	100.2	76.2	78.2	53.2	69.5	18.0
$\alpha$ -Rha2Me J	H	5.25	3.95	4.02	3.45	3.90	1.30
	C	100.2	75.9	75.4	71.8	69.5	18.0
$\alpha$ -PerN D	H	5.14	4.27	4.20	3.95	3.97	1.23
	C	100.1	67.4	75.2	52.2	69.4	18.0
$\alpha$ -Man E	H	5.13	4.17	3.99	3.75	3.84	
	C	100.1	70.9	79.8	67.1	74.4	
$\alpha$ -Man P	H	5.05	4.14	4.00	3.85	3.96	
	C	97.6	71.0	79.5	66.9	74.0	
$\beta$ -Rha U	H	4.78	4.16	3.69	3.48	3.44	1.32
	C	100.9	71.8	82.0	72.4	73.1	18.0
$\beta$ -Man Z"	H	4.72	4.06	3.75	3.75	3.46	3.83; 3.96
	C	98.2	71.9	86.0	67.0	77.4	62.1
$\beta$ -Man Z'	H	4.72	4.06	3.73	3.75	3.46	3.83; 3.96
	C	98.2	71.9	82.3	67.0	77.4	62.1

**Table 2.3:** NMR data for *C. crescentus* PS2 and its NaIO<sub>4</sub> oxidation product OS1 (40°C).

		1	2	3	4	5	6
$\alpha$ -Rha N, OS1	H	5.04	4.07	3.85	3.47	3.85	1.30
	C	103.1	71.1	71.1	72.9	69.9	17.6
$\alpha$ -Rha N, PS	H	5.02	4.02	3.79	3.45	3.72	1.28
	C	103.0	71.5	78.8	73.3	70.4	17.5
$\beta$ -Rha T, OS1	H	4.78	4.13	3.71	3.54	3.53	1.33
	C	100.7	71.1	72.3	83.4	71.7	17.5
$\beta$ -Rha T, PS	H	4.79	4.22	3.82	3.62	3.61	1.36
	C	101.7	76.7	73.5	83.4	73.2	17.5
$\beta$ -Rha V, OS1	H	4.75	4.12	3.67	3.49	3.49	1.34
	C	101.1	71.4	81.3	71.9	72.9	17.5
$\beta$ -Rha V, PS	H	4.77	4.13	3.66	3.66	3.50	1.35
	C	101.4	71.2	81.7	67.2	73.3	17.5
X (ox. G), OS1	H	3.69; 3.71	3.75	3.99	1.20		
	C	61.8	84.8	67.7	18.0		
$\alpha$ -Rha G, PS	H	5.10	4.13	3.94	3.58	3.90	1.35
	C	103.1	71.5	70.3	84.5		17.5
$\alpha$ -Rha F, PS	H	5.11	4.09	3.87	3.45	4.07	1.27
	C	102.4	72.1	71.3	73.3		17.5

**Table 2.4:** NMR data for the core oligosaccharide (25°C).

		1	2	3	4	5	6	7	8
Kdo C	H			2.05; 2.35	4.23	4.28	4.09	3.91	3.81; 3.93
	C	98.2	34.7	74.9	74.2	71.0	79.2		61.5
DLHep E	H	5.24	3.85	4.12	3.89	3.88	4.04	3.73; 3.73	
	C	101.1	80.2	71.1	67.3	74.1	70.0		63.9
Man F	H	5.03	4.30	4.00	3.79	3.80	3.80; 3.91		
	C	103.7	70.6	78.1	67.5	74.5	62.0		
DDHep G	H	5.15	4.05	3.86	3.77	3.84	4.06	3.76; 3.84	
	C	103.1	71.0	71.8	68.7	74.5	72.9		62.9
DLHep H	H	5.07	4.14	3.89	3.89	3.80	4.10	3.79; 3.81	
	C	102.7	73.7	71.8	67.3	73.2	70.2		64.9
GlcA K	H	5.22	3.66	4.00	3.99	4.15			
	C	98.8	72.4	74.9	73.6				
Gal L	H	5.49	3.80	3.85	3.99	3.94	3.69; 3.69		
	C	99.9	69.7	70.3	70.0	71.8	61.6		

# Bibliography

- [1] U. B. SLEYTR and P. MESSNER. Crystalline surface layers on bacteria. *Annual Reviews in Microbiology*, **37**: 311–339, 1983. (see p. 2)
- [2] P. MESSNER, D. PUM, and U. B. SLEYTR. Characterization of the ultrastructure and the self-assembly of the surface layer of *Bacillus stearothermophilus* strain NRS 2004/3a. *Journal of ultrastructure and molecular structure research*, **97**: 73–88, 1986. (see p. 1)
- [3] K. MASUDA and T. KAWATA. Reassembly of the regularly arranged subunits in the cell wall of *Lactobacillus brevis* and their reattachment to cell walls. *Microbiology and immunology*, **24**: 299–308, 1980. (see p. 1)
- [4] T. KAWATA and K. MASUDA. Extracellular crystalline lattice material of *Corynebacterium diphtheriae* revealed by electron microscopy. *Japanese journal of microbiology*, **16**: 515–523, 1972. (see p. 1)
- [5] E. ISHIGURO, W. KAY, T. AINSWORTH, J. CHAMBERLAIN, R. AUSTEN, J. BUCKLEY, et al. Loss of virulence during culture of *Aeromonas salmonicida* at high temperature. *Journal of bacteriology*, **148**: 333–340, 1981. (see p. 1)
- [6] R. L. WEISS. Subunit cell wall of *Sulfolobus acidocaldarius*. *Journal of bacteriology*, **118**: 275–284, 1974. (see p. 1)
- [7] In: (see p. 1)
- [8] S. HOLT and E. LEADBETTER. Comparative ultrastructure of selected aerobic spore-forming bacteria: a freeze-etching study. *Bacteriological reviews*, **33**: 346–378, 1969. (see p. 1)
- [9] J. SMIT, D. GRANO, R. GLAESER, and N. AGABIAN. Periodic surface array in *Caulobacter crescentus*: fine structure and chemical analysis. *Journal of bacteriology*, **146**: 1135–1150, 1981. (see p. 1)
- [10] A. HOUWINK. A macromolecular mono-layer in the cell wall of *Spirillum* spec. *Biochimica et biophysica acta*, **10**: 360–366, 1953. (see p. 4)
- [11] J. SMIT, I. A. KALTASHOV, R. J. COTTER, E. VINOGRADOV, M. B. PERRY, H. HAIDER, and N. QURESHI. Structure of a novel lipid A obtained from the lipopolysaccharide of *Caulobacter crescentus*. *Innate Immunity*, **14**: 25–36, 2008. (see pp. 5, 6)

- [12] S. G. WALKER, D. N. KARUNARATNE, N. RAVENSCROFT, and J. SMIT. Characterization of mutants of *Caulobacter crescentus* defective in surface attachment of the paracrystalline surface layer. *Journal of Bacteriology*, **176**: 6312–6323, 1994. (see pp. 5, 16, 19, 20)
- [13] P. AWRAM and J. SMIT. Identification of lipopolysaccharide O antigen synthesis genes required for attachment of the S-layer of *Caulobacter crescentus*. *Microbiology*, **147**: 1451–1460, 2001. (see pp. 5, 19, 20)
- [14] N. RAVENSCROFT, S. G. WALKER, G. G. DUTTON, and J. SMITH. Identification, isolation, and structural studies of the outer membrane lipopolysaccharide of *Caulobacter crescentus*. *Journal of Bacteriology*, **174**: 7595–7605, 1992. (see pp. 6, 16, 19)
- [15] N. RAVENSCROFT, S. G. WALKER, G. G. DUTTON, and J. SMIT. Identification, isolation, and structural studies of extracellular polysaccharides produced by *Caulobacter crescentus*. *Journal of Bacteriology*, **173**: Ravenscroft, N Walker, S G Dutton, G G Smit, J Research Support, Non-U.S. Gov't Research Support, U.S. Gov't, Non-P.H.S. United states Journal of bacteriology J Bacteriol. 1991 Sep;173(18):5677-84., 5677–5684, 1991. (see pp. 6, 14)
- [16] M. E. MARKS, C. M. CASTRO-ROJAS, C. TEILING, L. DU, V. KAPATRAL, T. L. WALUNAS, and S. CROSSON. The genetic basis of laboratory adaptation in *Caulobacter crescentus*. *Journal of Bacteriology*, **192**: 3678–3688, 2010. DOI: 10.1128/JB.00255-10 (see p. 14)
- [17] C. FARR, J. F. NOMELLINI, E. AILON, I. SHANINA, S. SANGSARI, L. A. CAVACINI, J. SMIT, and M. S. HORWITZ. Development of an HIV-1 Microbicide Based on : Blocking Infection by High-Density Display of Virus Entry Inhibitors. *PLoS One*, **8**: e65965, 2013. DOI: 10.1371/journal.pone.0065965PONE-D-12-33995[pii] (see p. 14)
- [18] F. AMAT, L. R. COMOLLI, J. F. NOMELLINI, F. MOUSSAVI, K. H. DOWNING, J. SMIT, and M. HOROWITZ. Analysis of the intact surface layer of *Caulobacter crescentus* by cryo-electron tomography. *Journal of Bacteriology*, **192**: 5855–5865, 2010. DOI: JB.00747-10[pii]10.1128/JB.00747-10 (see p. 14)
- [19] J. SMIT, M. HERMODSON, and N. AGABIAN. Caulobacter crescentus pilin. Purification, chemical characterization, and NH<sub>2</sub>-terminal amino acid sequence of a structural protein regulated during development. *Journal of Biological Chemistry*, **256**: 3092–3097, 1981. (see p. 15)
- [20] G. COHENBAZIRE, W. SISTROM, and R. STANIER. Kinetic studies of pigment synthesis by nonsulfur purple bacteria. *Journal of Cellular and Comparative Physiology*, **49**: 25–68, 1957. (see p. 15)
- [21] L. LEIVE. Release of lipopolysaccharide by EDTA treatment of *E. coli*. *Biochemical and biophysical research communications*, **21**: 290–296, 1965. (see p. 15)
- [22] R. P. DARVEAU and R. E. HANCOCK. Procedure for isolation of bacterial lipopolysaccharides from both smooth and rough *Pseudomonas aeruginosa* and *Salmonella typhimurium* strains. *Journal of Bacteriology*, **155**: 831–838, 1983. (see p. 16)

- [23] T. MANIATIS, E. F. FRITSCH, and J. SAMBROOK. *Molecular cloning: a laboratory manual*. vol. 545 Cold Spring Harbor, NY, 1982. (see p. 16)
- [24] E. G. BLIGH and W. J. DYER. A rapid method of total lipid extraction and purification. *Canadian journal of biochemistry and physiology*, **37**: 911–917, 1959. (see p. 17)
- [25] U. K. LAEMMLI. Cleavage of structural proteins during the assembly of the head of bacteriophage T4. *nature*, **227**: 680–685, 1970. (see p. 17)
- [26] Z.-X. ZHU, W.-T. CONG, M.-W. NI, X. WANG, W.-D. MA, W.-J. YE, L.-T. JIN, and X.-K. LI. An improved silver stain for the visualization of lipopolysaccharides on polyacrylamide gels. *Electrophoresis*, **33**: 1220–1223, 2012. DOI: 10.1002/elps.201100492 (see p. 17)
- [27] I. CIUCANU and F. KEREK. A simple and rapid method for the permethylation of carbohydrates. *Carbohydrate Research*, **131**: 209–217, 1984. (see p. 18)
- [28] H. BRADE. *Endotoxin in health and disease*. New York: Marcel Dekker, 1999. xviii, 950 p. (see p. 19)
- [29] Y. ZHANG, R. I. HOLLINGSWORTH, and U. B. PRIEFER. Characterization of Structural Defects in the Lipopolysaccharides of Symbiotically Impaired *Rhizobium-Leguminosarum* Biovar Viciae Vf-39 Mutants. *Carbohydrate Research*, **231**: 261–271, 1992. DOI: 10.1016/0008-6215(92)84024-M (see p. 19)
- [30] E. V. VINOGRADOV, K. BOCK, B. O. PETERSEN, O. HOLST, and H. BRADE. The structure of the carbohydrate backbone of the lipopolysaccharide from *Acinetobacter* strain ATCC 17905. *European Journal of Biochemistry*, **243**: 122–127, 1997. DOI: 10.1111/J.1432-1033.1997.0122a.X (see p. 19)
- [31] A. MOLL, S. SCHLIMPERT, A. BRIEGEL, G. J. JENSEN, and M. THANBICHLER. DipM, a new factor required for peptidoglycan remodelling during cell division in *Caulobacter crescentus*. *Molecular Microbiology*, **77**: 90–107, 2010. DOI: 10.1111/J.1365-2958.2010.07224.X (see p. 19)
- [32] L. E. METZGER IV, J. K. LEE, J. S. FINER-MOORE, C. R. RAETZ, and R. M. STROUD. LpxI structures reveal how a lipid A precursor is synthesized. *Nature structural molecular biology*, **19**: 1132–1138, 2012. (see p. 19)
- [33] J. B. THODEN, L. A. REINHARDT, P. D. COOK, P. MENDEN, W. CLELAND, and H. M. HOLDEN. Catalytic Mechanism of Perosamine N-Acetyltransferase Revealed by High-Resolution X-ray Crystallographic Studies and Kinetic Analyses. *Biochemistry*, **51**: 3433–3444, 2012. (see p. 19)
- [34] M. T. CABEEN, M. A. MUROLO, A. BRIEGEL, N. K. BUI, W. VOLLMER, N. AUSMEES, G. J. JENSEN, and C. JACOBS-WAGNER. Mutations in the lipopolysaccharide biosynthesis pathway interfere with crescentin-mediated cell curvature in *Caulobacter crescentus*. *Journal of Bacteriology*, **192**: 3368–3378, 2010. (see p. 19)
- [35] C. R. H. RAETZ and C. WHITFIELD. Lipopolysaccharide endotoxins. *Annual Review of Biochemistry*, **71**: 635–700, 2002. DOI: 10.1146/Annurev.Biochem.71.110601.135414 (see p. 20)

# **Appendix A**

## **Supporting Materials**

This would be any supporting material not central to the dissertation. For example:

- Authorizations from Research Ethics Boards for the various experiments conducted during the course of research.
- Copies of questionnaires and survey instruments.